frontiers | Frontiers in Physics

TYPE Original Research
PUBLISHED 07 October 2022
DOI 10.3389/fphy.2022.1034973

Check for updates

OPEN ACCESS

EDITED BY
Zhenxu Bai,
Hebei University of Technology, China

REVIEWED BY
Yaoyao Qi,
Hebei University of Technology, China
Bo Guo,
Harbin Engineering University, China

*CORRESPONDENCE
Bingyuan Zhang,
bingyuanzhang@lcu.edu.cn

SPECIALTY SECTION
This article was submitted to Optics and Photonics,
a section of the journal
Frontiers in Physics

RECEIVED 02 September 2022
ACCEPTED 20 September 2022
PUBLISHED 07 October 2022

CITATION
Liu C, Li G, Su X, Wang Y, Gao F, Xie Y, Kumar S and Zhang B (2022), Generation of h–Shaped pulse in a mode–Locked erbium-doped fiber laser.
Front. Phys. 10:1034973.
doi: 10.3389/fphy.2022.1034973

COPYRIGHT
© 2022 Liu, Li, Su, Wang, Gao, Xie, Kumar and Zhang. This is an open-access article distributed under the terms of the Creative Commons Attribution License (CC BY). The use, distribution or reproduction in other forums is permitted, provided the original author(s) and the copyright owner(s) are credited and that the original publication in this journal is cited, in accordance with accepted academic practice. No use, distribution or reproduction is permitted which does not comply with these terms.

Generation of h–Shaped pulse in a mode–Locked erbium-doped fiber laser

Chao Liu, Guoru Li, Xiancui Su, Yiran Wang, Feilong Gao, Yiyan Xie, Santosh Kumar and Bingyuan Zhang*

Shandong Key Laboratory of Optical Communication Science and Technology, School of Physics Science and Information Technology, Liaocheng University, Liaocheng, China

In this paper, the generation of h-shaped pulse is demonstrated in a nonlinear polarization rotation mode-locked erbium-doped fiber laser (MLEDFL). The length of the entire cavity is about 2506 m to enhance the nonlinear effect in the cavity. The multi-pulse state is obtained firstly under the certain pump power and polarization state. By further adjusting the polarization controller the h-shaped pulse with sharp top and flat bottom is generated under the pump power of ~100 mW. And the duration of pulse is tuned with a range of 54.63–470 ns. The width and intensity of pulse trailing part vary differently during the process of increasing pulse width. The results indicate that the peak power clamping effect and weak birefringence effect dominate in different h-shaped pulse forming process.

KEYWORDS

h-shaped pulse, ultra-long cavity, mode-locked, fiber laser, nonlinear effect

Introduction

Passively mode-locked fiber lasers (MLFLs) have attracted a lot of interest in the area of academia and industry in recent decades, for instance, optical sensing [1, 2], materials micromachining [3, 4] and biomedicine [5]. A strong nonlinear effect exists in MLFLs as a result of the unique structure of the fiber core. And the complex dynamic processes occur in fiber lasers under the action of nonlinear effects. Therefore, various pulse shapes will be generated from passively MLFLs, for example bunched multi-solitons [6], rectangular-wave pulses [7–9], step-like pulses [10, 11], chair-like pulses [12, 13], and h-shaped pulses [14, 15].

In 1991, the square pulse was firstly observed by Richardson based on figure-eight passively MLFLs [16]. The features of rectangular-wave pulses, however, have not been fully investigated. Komarov et al. theoretically researched the dynamics of the rectangular-wave pulses in an NPR fiber laser subsequently [17]. The mechanism for suppressing the formation of additional pulses was established based on numerical simulation in a laser resonator as pump power increased [18]. Since then, more and more researchers have begun to study the rectangular-wave pulse in fiber lasers. Zhang realized the rectangular-wave pulse with tuning range of 10–1710 ns by enhancing intracavity nonlinearity and cavity length [8]. The results show that the stronger nonlinearity in the cavity has a

positive impact on the pulse duration. Liu reported that the multiwavelength square pulses were generated by utilizing a NALM-based cavity filtering effect in a passively MLFL with anomalous dispersion using a figure-eight structure [19]. The results indicate that as pump power increases, the width of rectangular-wave pulses broadens linearly, yet the peak power remains practically constant.

In addition to rectangular-wave pulses, another h-shaped pulse has also drawn a lot of interest in a unique structure with a sharper peak on the leading edge and a longer flat-top bunch on the trailing edge. In 2018, Luo found that the h-shaped pulses as the pump source could realize high repetition gain-switching [14]. In the same year, Zhao investigated the influences of weak birefringence in the cavity on pulse characteristics [20]. In 2019, Zheng demonstrated that nanoscale h-shaped pulses with μJ-level pulse energy could be generated in the figure-of-9 fiber laser [21]. The generation of h-shaped pulse was realized by Zhao by employing an ultralong fiber laser resonator, revealing that by increasing pump power or varying intra-cavity polarization state, the h-shaped pulse could be generated with different orders of harmonic mode-locking state [15]. Compared to low-dimensional material SAs [22], nonlinear multimode interference (NLMMI) [23, 24] mode-locked technology, the mode-locked principle of NPR is based on the accumulation of different nonlinear phase shifts in the cavity. And the strong nonlinear effect is conducive to reducing the nonlinear polarization switching threshold, which means that it is easy to obtain h-type pulses at lower pump power.

In this work, the evolution of h-shaped pulse is demonstrated in a passively MLEDFL based on NPR technique. By varying the polarization, the h-shaped pulses can be switched from the multi-pulse state under the fixed pump power. The pump power varies from 100 mW to 350 mW, and the pulse width changes from 54.63 to 470 ns. The width and intensity of the pulse trailing part change during the process of pulse width increase. The results indicate that the peak power clamping effect and weak birefringence effect dominate in different h-shaped pulse forming processes. It may be helpful to further enhance understanding the physical properties of the h-shaped pulses which generate in MLFLs.

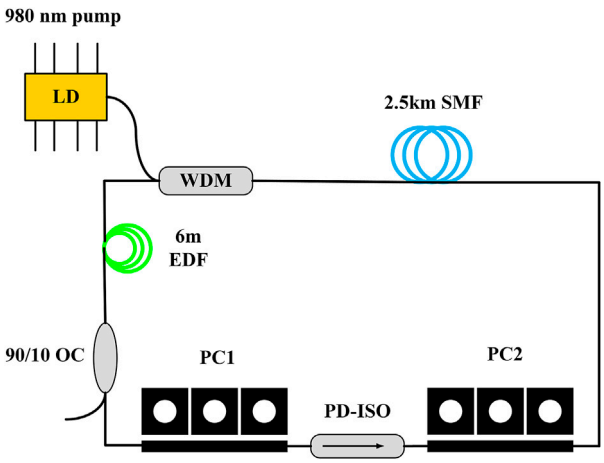

FIGURE 1
Schematic diagram of the MLFL based on NPR technique.

Experimental setup

The experimental schematic diagram of the passively MLFL is shown in Figure 1. The length of the entire cavity is around 2506 m. The erbium-doped fiber (EDF, 4/125 μm) as gain medium is pumped by a 980 nm laser diode (LD) through a 980/1550 nm wavelength division multiplexed (WDM) coupler. The Er-doped fiber is low-gain fiber, so we use the length of 6 m Er-doped fiber as the gain fiber. The cavity length of 2506m is to increase the nonlinear effect in the cavity and reduce the nonlinear polarization switching threshold, so as to achieve a wide range h-shaped pulse output in time domain. The optical coupler (OC) is used to extract 10% of the power from the cavity.

Two three-paddle type polarization controllers (PC1 and PC2) are used to adjust the polarization state of the propagation light. In addition, the polarization-dependent isolator (PD-ISO) is used to ensure the unidirectional transmission in the ring cavity. A 2.5 km long single mode fiber (SMF) is added to the cavity to prolong the cavity length and enhance the cumulative nonlinearity. The temporal pulse profile and output spectrum are monitored by using a 1 GHz digital oscilloscope (Tektronix MDO3102) and an optical spectrum analyzer with a scanning range of 600–1700 nm (Yokogawa AQ6370), respectively. The net dispersion of the ring cavity is calculated to be -53.87 ps^2.

Results and analysis

In our experiment, with launched pump power fixed at 100 mW, three tight pulses emerge from the laser cavity by altering the PCs properly. Figures 2A,B illustrate the temporal profile of the pulse and optical spectrum, respectively. It can be observed the temporal distance between adjacent pulses is not equidistant and interval is large, showing that the interaction of the pulse is weak. The whole output spectrum is broad with no Kelly sideband features of conventional-soliton pulse. And the central wavelength is located at 1573 nm with ~23 nm 3 dB spectral bandwidth.

Figures 3A,B illustrate the evolution of the number of round-trip pulses and the output spectra with increasing pump power, respectively, to further examine the behaviors of multi-pulses in MLFL. The intensity of the output spectrum enhances slightly with the increase of pump power. The corresponding number of the round-trip pulses varies from

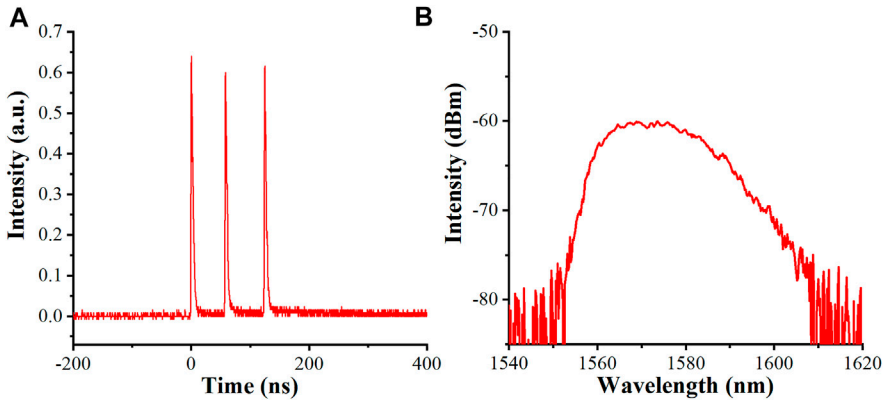

FIGURE 2
(A) The temporal pulse profile of the three pulses. **(B)** The corresponding optical spectrum.

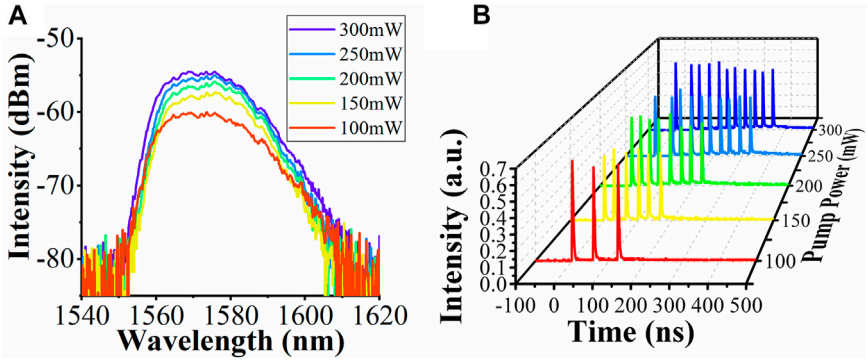

FIGURE 3
The evolution of **(A)** the output spectra and **(B)** the temporal pulse profile with increasing pump powers.

6 to 11, during the pump power increases to 300 mW. The temporal spacing between adjacent pulses is not equivalent, but the shape and width of pulses are essentially uniform. This is because gain competition between neighboring pulses and experimental ambient noise may induce pulse intensity inconsistency [25]. It is similar to the harmonic mode-locked (HML) regime in that the excess energy in the cavity is converted to build up the number of pulses. In fact, the operation of multi-pulses in NPR MLFLs can be attributed to weakly birefringent effects in optical fiber, gain dynamics, and nonlinearity [20].

The h-shaped pulse is obtained at the pump power of ~100 mW by slightly adjusting the PC again. Figures 4A,B show the output spectra and temporal profiles, respectively. It can be observed that there are dual central bands in the output spectrum. The first band has a central wavelength and a 3 dB spectral bandwidth of 1543.5 nm and 3 nm, respectively. The second band has a central wavelength and a 3 dB spectral bandwidth of 1585 nm and 28 nm, respectively. The second segment has a wider spectrum with a depression in the center. The birefringence-related cavity-spectral-filtering (CSF) effect may be the reason why two independent spectra bands appear [20]. According to Ref. [26], there is a strong correlation between the time and spectral distribution of the J-shaped pulse. In this experiment, the intensity of the leading edge and the trailing edge of the h-shaped pulse is almost the same, meaning that the same effect on the wider spectrum. Although the ultra-long SMF cumulates the intracavity nonlinearity, it also increases intracavity birefringence, which changes the CFS effect related to the birefringence. Figure 4C shows the corresponding pulse train at 100 mW of pumping power, which corresponds to a repetition rate of 81.17 kHz. Meanwhile, the measured RF spectrum in the

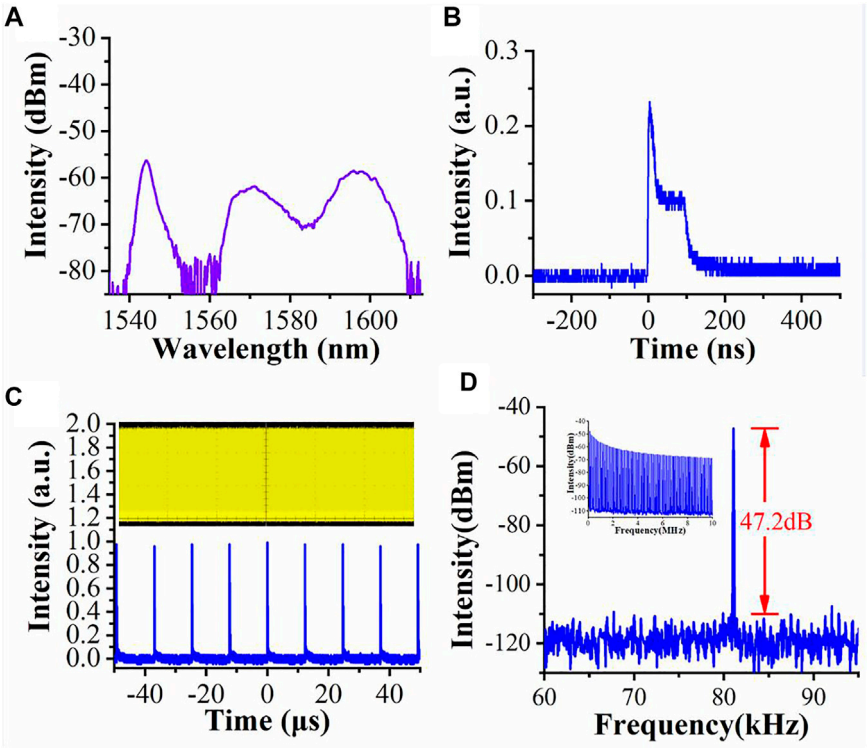

FIGURE 4
Output characteristics of the h-shaped pulse with ~100 mW pump power: **(A)** output spectra; **(B)** temporal profile; **(C)** pulse train (inset: a span of 1 ms); **(D)** the RF spectrum (insert: RF spectrum in 10 MHz range).

range of 0–10 MHz confirms that the operation of mode-locked has excellent stability.

Figure 5B shows the evolution of the h-shaped pulse at different pump powers. The pulse width ranges from 94 to 292 ns as the pump power increases from 100 to 240 mW. As the pump power increases, the peak power of the pulse does not increase due to the clamping effect, but the gain is not saturated so the pulse width can increase continuously. The flat trailing portion broadens as pump power increases, while the sharp spike of the pulse narrows slowly. This is similar to the properties of dissipative soliton resonance (DSR) pulse in fiber lasers [27, 28]. It is noteworthy that the repetition frequency of the mode-locked pulse is 81kHz, it is not so easy to induce amplified spontaneous emission (ASE) in the pulse interval. So, the properties of trailing portion are just caused by the peak power clamping (PPC) effect rather ASE. The PPC effect contributes to the formation of h-shaped pulses and inhibits pulse splitting by flattening the lengthy trailing section [15]. Meanwhile, the PPC effect is associated with the nonlinearity in the laser resonant cavity, which implies the intensive nonlinearity can reduce the switching threshold [29]. As seen in Figure 5A, the intensity of corresponding output spectra increases slightly as the pump power increases, while the central wavelength remains almost invariable, which is consistent with the previously proven features of an h-shaped pulse [14, 20, 30, 21, 15]. As the pump power reaches 240 mW, the temporal pulse profile becomes unstable. Then, we rotate the PCs slightly, and the mode-locked pulse reappears again. Figures 5C,D, respectively, display the output spectra and temporal pulse profile. It is found that the central wavelength of the optical spectrum has changed. The band has a central wavelength of 1572 nm. The measured pulse duration widens from 368 to 470 ns as the pump power changes from 260 to 340 mW. And the complete pulse profile is observed by adjusting the vertical resolution of the oscilloscope. It can be seen the amplitude of sharp peak is higher than previously mentioned, the amplitude of trailing portion remains almost invariant. Theoretically, rotating the PCs will change the local birefringence of the fiber, resulting in a change in the amount of intracavity birefringence and further impacting the characteristics of the output pulse [20]. For the h-shape pulse with higher amplitude of sharp peak, the PPC effect plays a weak role in the formation of sharp peak, but it contributes to inhibit pulse splitting by flattening the lengthy trailing section. The energy of whole pulse is more

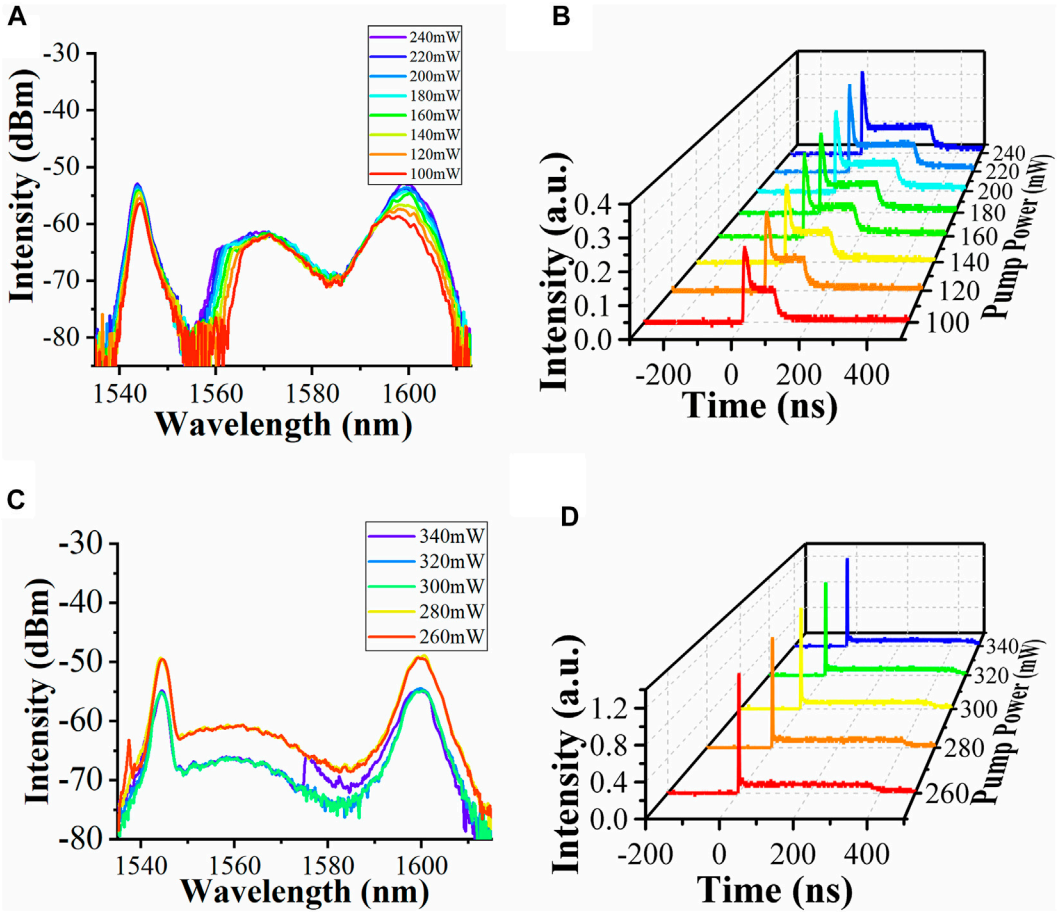

FIGURE 5
(A) Output spectra and **(B)** the temporal pulse profile variations *versus*versus different pump powers. **(C)** Changes of the spectra after adjusting the PCs and **(D)** the corresponding variations of the temporal pulse profile.

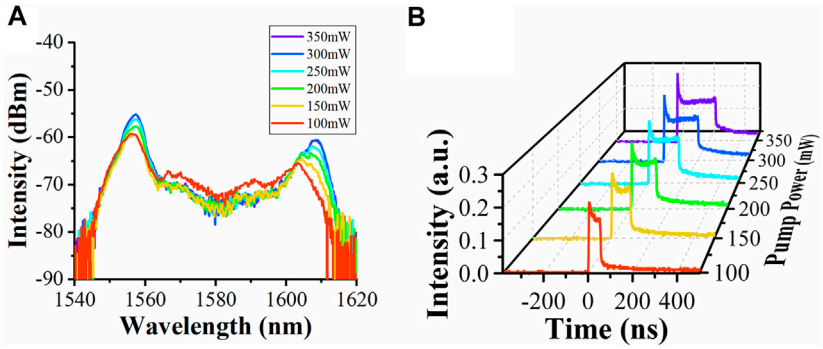

FIGURE 6
(A) The variations of the output spectra under different pump powers after adjusting the PCs. **(B)** Corresponding temporal pulse profile as increasing pump power.

concentrated on the peak of pulse instead of splitting into pulses with the same power.

In order to further investigate the characteristics of the h-shaped pulse, another h-shaped pulse is generated by rotating the angle of the PCs. Figures 6A,B show the output spectra and the corresponding temporal pulse profile as increasing pump power respectively. The corresponding pulse width ranges from 54.63 to 245.9 ns as the pump power increases from 100 to 350 mW. The output spectrums have changed, and the central wavelength reduced from two to one, which can be attributed to the different intensity of CSF effect caused by the angle of PCs. As can be noticed, there are no-Signiant change with the amplitude of the flat-top portion. According to Ref. [30], it could be found that the sharp peak at the top of an h-shaped pulse might be restrained by inserting a piece of unpumped doped-fiber into the cavity. Similarly, this function can be realized by adjusting the PC in this experiment. It may be helpful to further enhance understanding the physical properties of the h-shaped pulses in MLFLs.

Conclusion

In conclusion, the evolution of h-shaped pulses in an ultralong NPR MLEDFL is experimentally realized. The 2.5 km long SMF is employed in the cavity to enhance the nonlinear effect. By adjusting the polarization, the h-shaped pulse can evolve from the multi-pulse state. And the duration of pulse is tuned with a range of 54.63–470 ns. The width and intensity of pulse trailing part vary differently during the process of increasing pulse width. The results indicate that the peak power clamping effect and weak birefringence effect dominate in different h-shaped pulse forming process. The experimental results may be helpful to investigate the output performances of the h-shaped pulse in MLEDFLs.

Data availability statement

The original contributions presented in the study are included in the article/supplementary material, further inquiries can be directed to the corresponding author.

Author contributions

All authors listed have made a substantial, direct, and intellectual contibution to the work and approved it for Publication.

Funding

Natural Science Foundation of Shandong Province (ZR2021QF025, ZR2020QF093); National Natural Science Foundation of China (62105134, 61905104).

Conflict of interest

The authors declare that the research was conducted in the absence of any commercial or financial relationships that could be construed as a potential conflict of interest.

Publisher's note

All claims expressed in this article are solely those of the authors and do not necessarily represent those of their affiliated organizations, or those of the publisher, the editors and the reviewers. Any product that may be evaluated in this article, or claim that may be made by its manufacturer, is not guaranteed or endorsed by the publisher.

References

1. Zhao X, Hu G, Zhao B, Li C, Pan Y, Liu Y, et al. Picometer-resolution dual-comb spectroscopy with a free-running fiber laser. *Opt Express* (2016) 24(19): 21833–45. doi:10.1364/oe.24.021833

2. Cao Y, Wang L, Lu Z, Wang G, Wang X, Ran Y, et al. High-speed refractive index sensing system based on Fourier domain mode locked laser. *Opt Express* (2019) 27(6):7988–96. doi:10.1364/oe.27.007988

3. Kerse C, Kalaycıoğlu H, Elahi P, Çetin B, Kesim DK, Akçaalan Ö, et al. Ablationcooled material removal with ultrafast bursts of pulses. *Nature* (2016) 537(7618):84–8. doi:10.1038/nature18619

4. Malinauskas M, Žukauskas A, Hasegawa S, Hayasaki Y, Mizeikis V, Buividas R, et al. Ultrafast laser processing of materials: From science to industry. *Light Sci Appl* (2016) 5(8):e16133. doi:10.1038/lsa.2016.133

5. Wilson CR, Hutchens TC, Hardy LA, Irby PB, Fried NM. A miniaturized, 1.9F integrated optical fiber and stone basket for use in thulium fiber laser lithotripsy. *J Endourol* (2015) 29(10):1110–4. doi:10.1089/end.2015.0124

6. Chen Y, Wu M, Tang P, Chen S, Du J, Jiang G, et al. The formation of various multi-soliton patterns and noise-like pulse in a fiber laser passively mode-locked by a topo-logical insulator based saturable absorber. *Laser Phys Lett* (2014) 11:055101. doi:10.1088/1612-2011/11/5/055101

7. Li S, Dong Z, Li G, Chen R, Gu C, Xu L, et al. Chirp-adjustable square-wave pulse in a passively mode-locked fiber laser. *Opt Express* (2018) 26(18):23926–34. doi:10.1364/oe.26.023926

8. Zhang X, Gu C, Chen G, Sun B, Xu L, Wang A, et al. Square-wave pulse with ultra-wide tuning range in a passively mode-locked fiber laser. *Opt Lett* (2012) 37(8):1334–6. doi:10.1364/ol.37.001334

9. Semaan G, Braham FB, Fourmont J, Salhi M, Bahloul F, Sanchez F. 10 μJ dissipative soliton resonance square pulse in a dual amplifier figure-of-eight double-clad Er:Yb mode-locked fiber laser. *Opt Lett* (2016) 41(20):4767–70. doi:10.1364/ol.41.004767

10. Mao D, Liu X, Wang L, Lu H, Duan L. Dual-wavelength step-like pulses in an ultra-large negative-dispersion fiber laser. *Opt Express* (2011) 19(5):3996–4001. doi:10.1364/oe.19.003996

11. Guo B, Yao Y, Xiao J, Wang R, Zhang J. Topological insulator-assisted dual-wavelength fiber laser delivering versatile pulse patterns. *IEEE J Sel Top Quan Electron* (2016) 22(2):0900108–15. doi:10.1109/jstqe.2015.2426951

12. Dong Z, Lin J, Li H, Li S, Tao R, Gu C, et al. Generation of mode-locked square-shaped and chair-like pulse based on reverse saturable absorption effect of nonlinear multimode interference. *Opt Express* (2019) 27(20):27610–7. doi:10.1364/oe.27.027610

13. Gupta PK, Singh CP, Singh A, Sharma SK, Mukhopadhyay PK, Bindra KS. Chair-like pulses in an all-normal dispersion Ytterbium-doped mode-locked fiber laser. *Appl Opt* (2016) 55(35):9961–7. doi:10.1364/ao.55.009961

14. Luo H, Liu F, Li J, Liu Y. High repetition rate gain-switched Ho-doped fiber laser at 2.103 μm pumped by h-shaped mode-locked Tm-doped fiber laser at 1.985 μm. *Opt Express* (2018) 26(20):26485–94. doi:10.1364/oe.26.026485

15. Zhao J, Li L, Zhao L, Tang D, Shen D, Su L. Tunable and switchable harmonic h-shaped pulse generation in a 3.03 km ultralong mode-locked thulium-doped fiber laser. *Photon Res* (2019) 7(3):332–40. doi:10.1364/prj.7.000332

16. Richardson DJ, Laming RI, Payne DN, Matsas V, Phollips MW. Selfstarting, passively modelocked erbium fibre ring laser based on the amplifying Sagnac switch. *Electron Lett* (1991) 27:542. doi:10.1049/el:19910341

17. Komarov A, Leblond H, Sanchez F. Multistability and hysteresis phenomena in passively mode-locked fiber lasers. *Phys Rev A (Coll Park)* (2005) 71(5):053809. doi:10.1103/physreva.71.053809

18. Komarov A, Amrani F, Dmitriev A, Komarov K, Sanchez F. Competition and coexistence of ultrashort pulses in passive mode-locked lasers under dissipative-soliton-resonance conditions. *Phys Rev A (Coll Park)* (2013) 87(2):023838. doi:10.1103/physreva.87.023838

19. Liu H, Zheng X, Zhao N, Ning Q, Liu M, Luo Z, et al. Generation of multiwavelength noise-like square-pulses in a fiber laser. *IEEE Photon Technol Lett* (2014) 26(19):1990–3. doi:10.1109/lpt.2014.2344505

20. Zhao J, Li L, Zhao L, Tang D, Shen D. Cavity-birefringence-dependent h-shaped pulse generation in a thulium-holmium-doped fiber laser. *Opt Lett* (2018) 43(2):247–50. doi:10.1364/ol.43.000247

21. Zheng Z, Ren X, Zhu K, Ouyang D, Wang J, Guo C, et al. Fundamental and harmonic mode-locked h-shaped pulse generation using a figure-of-9 thulium-doped fiber laser. *Opt Express* (2019) 27(26):37172–9. doi:10.1364/oe.27.037172

22. Qi YY, Yang S, Wang JJ, Li L, Bai ZX, Wang YL, et al. Recent advance of emerging low-dimensional materials for vector soliton generation in fiber lasers. *Mater Today Phys* (2022) 23:100622. doi:10.1016/j.mtphys.2022.100622

23. Qi YY, Zhang Y, Yang S, Bai ZX, Ding J, Wang YL, et al. Controllable multiple-pulse dynamic patterns in the mode-locking ultrafast laser with a GIMF-YDF-based saturable absorber. *Opt Laser Tech* (2022) 153:108274. doi:10.1016/j.optlastec.2022.108274

24. Qi YY, Liu MY, Luan NN, Yang S, Bai ZX, Yan BZ, et al. Recent research progress of nonlinear multimode interference mode-locking technology based on multimode fibers. *Infrared Phys Tech* (2022) 121:104017. doi:10.1016/j.infrared.2021.104017

25. Kokhanovskiy A, Kuprikov E, Kobtsev S. Single- and multi-soliton generation in figure-eight mode-locked fibre laser with two active media. *Opt Laser Technol* (2020) 131:106422. doi:10.1016/j.optlastec.2020.106422

26. Gupta PK, Singh CP, Mukhopadhyay PK, Bindra KS. Generation of J-shaped pulses in ultra-long Ytterbium doped mode locked fiber laser. *Laser Phys* (2022) 30(6):065105. doi:10.1088/1555-6611/ab8797

27. Chang W, Ankiewicz A, Soto-Crespo JM, Akhmediev N. Dissipative soliton resonances. *Phys Rev A (Coll Park)* (2008) 78(2):023830. doi:10.1103/physreva.78.023830

28. Wu X, Tang DY, Zhang H, Zhao LM. Dissipative soliton resonance in an all-normal-dispersion erbium-doped fiber laser. *Opt Express* (2009) 17(7):5580–4. doi:10.1364/oe.17.005580

29. Li G, Liu J, Wang F, Nie H, Wang R, Yang K, et al. Third-order nonlinear optical response of few-layer MXene Nb_2C and applications for square-wave laser pulse generation. *Adv Mater Inter* (2021) 8(6):2001805. doi:10.1002/admi.202001805

30. Zhao J, Zhou J, Li L, Klimczak M, Komarov A, Su L, et al. Narrow-bandwidth h-shaped pulse generation and evolution in a net normal dispersion thulium-doped fiber laser. *Opt Express* (2019) 27(21):29770–80. doi:10.1364/oe.27.029770